Theoretical and Experimental Investigation of the Stability Limits of Quinones in Aqueous Media: Implications for Organic Aqueous Redox Flow Batteries

Daniel P. Tabor[#,†] Rafael Gómez-Bombarelli[#,†,‡] Liuchuan Tong,[†] Roy G. Gordon,[†,¶] Michael J. Aziz,[¶] and Alán Aspuru-Guzik[*,†,§,‖]

†*Department of Chemistry and Chemical Biology, Harvard University, Cambridge, MA 02138 USA*

‡*Present Address: Department of Materials Science and Engineering, Massachusetts Institute of Technology, Cambridge, MA 02139 USA*

¶*Harvard John A. Paulson School of Engineering and Applied Sciences, Cambridge, Massachusetts 02138 USA*

§*Senior Fellow, Canadian Institute for Advanced Research, Bioinspired Solar Energy Program, Toronto, ON M5G 1Z8, Canada*

‖*Present Address: Department of Chemistry and Department of Computer Science, University of Toronto, Toronto, Ontario M5S 3H6, Canada and Vector Institute, Toronto, ON M5G 1M1, Canada.*

E-mail: alan@aspuru.com

[#]These authors contributed equally.

Abstract

Quinone-hydroquinone pairs have been proposed as biologically-inspired, low-cost redox couples for organic electrolytes for electrical energy storage, particularly in aqueous redox flow batteries. In their oxidized form, quinones are electrophiles that can react with the nucleophilic water solvent resulting in loss of active electrolyte. Here we study two mechanisms of nucleophilic addition of water, one reversible and one irreversible, that limit quinone performance in practical flow batteries. Using a combination of density functional theory and semi-empirical calculations, we have quantified the source of the instability of quinones in water, and explored the relationships between chemical structure, electrochemical reduction potential, and decomposition or instability mechanisms. By combining these computational estimates with the experimental study of the aqueous stability of alizarin-derived quinones, quantitative thresholds for chemical stability of oxidized quinones were established. Finally, ∼140,000 prospective quinone pairs (over 1,000,000 calculations including decomposition products) were analyzed in a virtual screening using the learned design principles. Our conclusions suggest that numerous low reduction potential molecules are stable with respect to nucleophilic addition, but promising high reduction potential molecules are much rarer. This latter fact suggests the existence of a stability cliff for this family of quinone-based organic molecules, which challenges the development of all-quinone aqueous redox flow batteries.

Keywords. Quinone flow battery, organic molecule stability, high-throughput virtual screening

Introduction

Flow batteries could help solve the intermittency problem of wind and solar renewable sources by storing electrical energy in fluids in scalable external storage tanks. Research into low-

cost alternatives to current-standard vanadium electrolytes has exploded in the past five years, with organic, inorganic, and organometallic electrolytes developed for both aqueous and non-aqueous systems.[1–16] For aqueous flow batteries, the vast majority of developments have been new molecules for the low reduction potential electrolyte (the negolyte), with the molecule for the high-potential electrolyte (the posolyte) serving as a greater challenge. Some success has been found using single-electron couples at neutral and high-pH.[3–5,9,10] Initial work in acidic aqueous metal-free flow batteries used bromine as the posolyte active species[2] and two recent studies used benzoquinone-based molecules.[6,8] However, the maximum standard reduction potential for an acidic organic posolyte that has lasted even a few cycles (3,6-dihydroxy-2,4-dimethylbenzene sulfonic acid or DHDMBS) is only 0.85 V vs. the standard hydrogen electrode (SHE)–this is almost 0.4 V below the thermodynamic threshold for evolving oxygen.[8] In addition to the need to develop high potential molecules, there is also interest in developing single molecules with three distinct, well separated (> 1.0 V) redox states, that could potentially serve in both posolyte and negolyte. Discovering molecules with this property could enable flow batteries that replace the ion-selective membrane with an inexpensive porous separator.[17–19] One potential three-redox-state molecule is a fused quinone, which contains four total ketone groups.

A primary concern in developing flow battery electrolytes is their chemical and electrochemical stability. Organic molecules are subject to a variety of decomposition reactions, which vary across different backbones, functionalizations, and environments. Previous studies have investigated the susceptibility of quinones to reactions with bromine[20] and a Michael-addition mechanism has been proposed for their reactions with water.[6,8,17]

Here, we present a combined theoretical and experimental study of the structure-property relationships relating to stability of a family of quinones. A comprehensive library of quinone-derived molecules (with backbones shown in Scheme 1A), containing 146,857 hydroquinone pairs and associated products from reactions with water, is screened.[4,21,22] The targets are high (or low) reduction potential and high thermodynamic stability with respect to water

attack. The experimental component focuses on the comprehensive study of a family of fused quinones and provides full characterization of the decomposition products. When coupled with theoretical calculations of the relevant reaction energies of decomposition reactions, this provides a firm target for which to virtually screen. These results, taken together, show the tradeoffs between achieving a high reduction potential quinone and maintaining long-term stability.

The molecular backbones and mechanisms of decomposition reactions that we considered are summarized in Scheme 1. The two-proton two-electron redox activity of a molecule (Scheme 1B) can be kinetically inhibited by the formation of a gem-diol (Scheme 1C) and the molecule can undergo chemical degradation through a Michael addition or substitution reaction (Scheme 1D).

Reduction potential structure-property relationships

The choice of candidate quinone pool was based on previous reports,[21] where molecular motifs more likely to give high reduction potentials and high solubility have been identified. The molecules were generated as fully reduced parts of redox pairs and subject to two-proton, two-electron oxidation reactions. Figure 1 plots the distribution of the calculated reduction potentials vs. SHE at pH = 0 for the benzoquinones, naphthoquinones, anthraquinones, and phenanthrene-functionalized quinones across the three main functional groups considered in this study: carboxylic acids, sulfonic acids, and phosphonic acids. These results are calculated at the calibrated PM7 COSMO level of theory.[23,24] Details on the on the calibration procedure and the calibration results for higher levels of theory are given at the end of the manuscript and in the supplementary material (Figure S1). Within each distribution, there are variations in the hydroxyl substitutions for the non redox-active parts of the molecules and the number and positioning of the other functional groups. For hydroquinones with multiple potential oxidation patterns, all mechanisms have been considered, and results are reported for the reaction with the highest thermodynamic driving force.

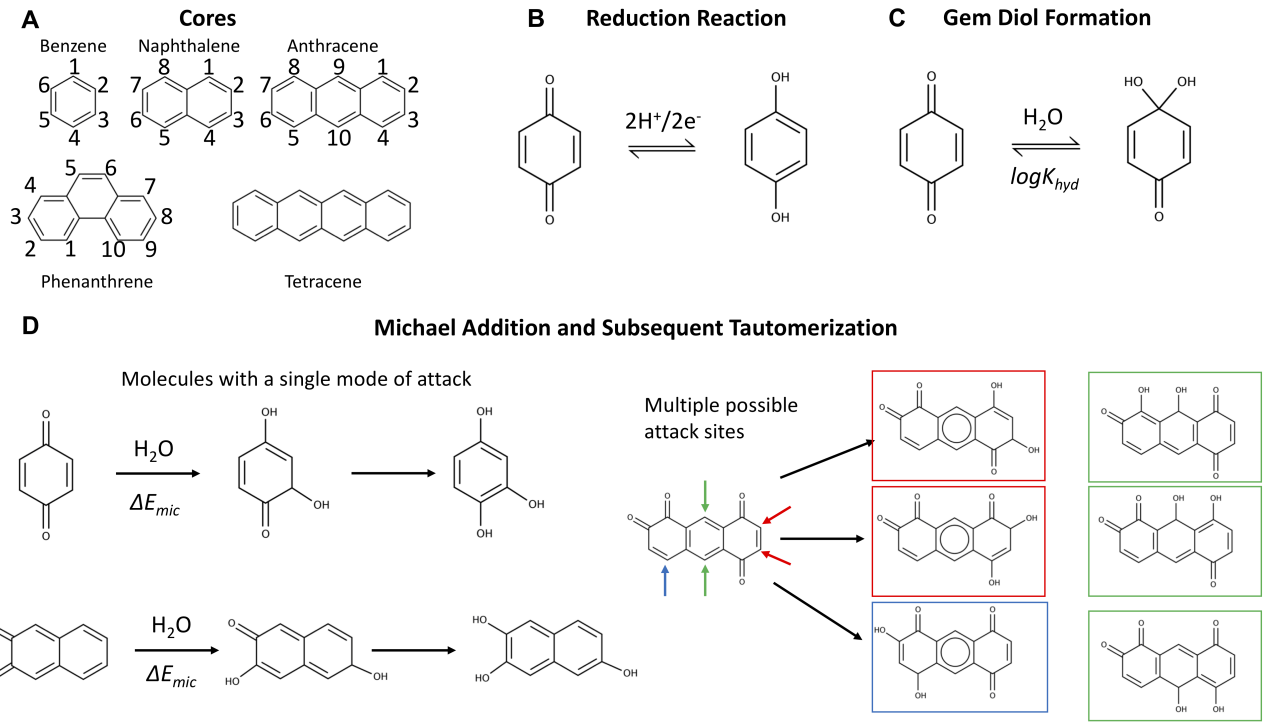

Scheme 1: A) All backbones (without oxidation topologies indicated) considered in this study. The molecules discussed in detail are labeled to give a short description of the redox-active sites in a given molecule. B) The redox reaction of quinones in acidic aqueous flow batteries: the two-proton two-electron reduction of two ketones to two hydroxyl groups C) Mechanism for gem-diol formation, which is reversible but hampers kinetics. D) Illustrations of Michael addition (irreversible) on molecules with a single vulnerable site (with subsequent tautomerization shown) and on molecules with multiple vulnerable attack sites. Michael addition can also occur on substituted sites, where it becomes a substitution reaction.

In general, the redox pattern, also referred to as the relative positions of the redox-active hydroxyl groups, has the strongest influence over reduction potential; this is most easily seen by examining the median values in Figure 1. The choice of electron withdrawing group has a slightly weaker effect, particularly for the larger backbones. Also of note is that essentially every redox pattern and functional group combination is capable of producing quinones with both high potentials (near $\sim$1.00 V) and low potentials ($\sim$0.1 V). Overall, the theoretical methods predict that carboxylic acid and sulfonic acid functionalizations lead to higher reduction potentials within a given redox-active pattern.

For the benzoquinones (Figure 1A) and naphthoquinones (Figure 1B), there is not as large of a difference between the medians of the different redox-active patterns as there

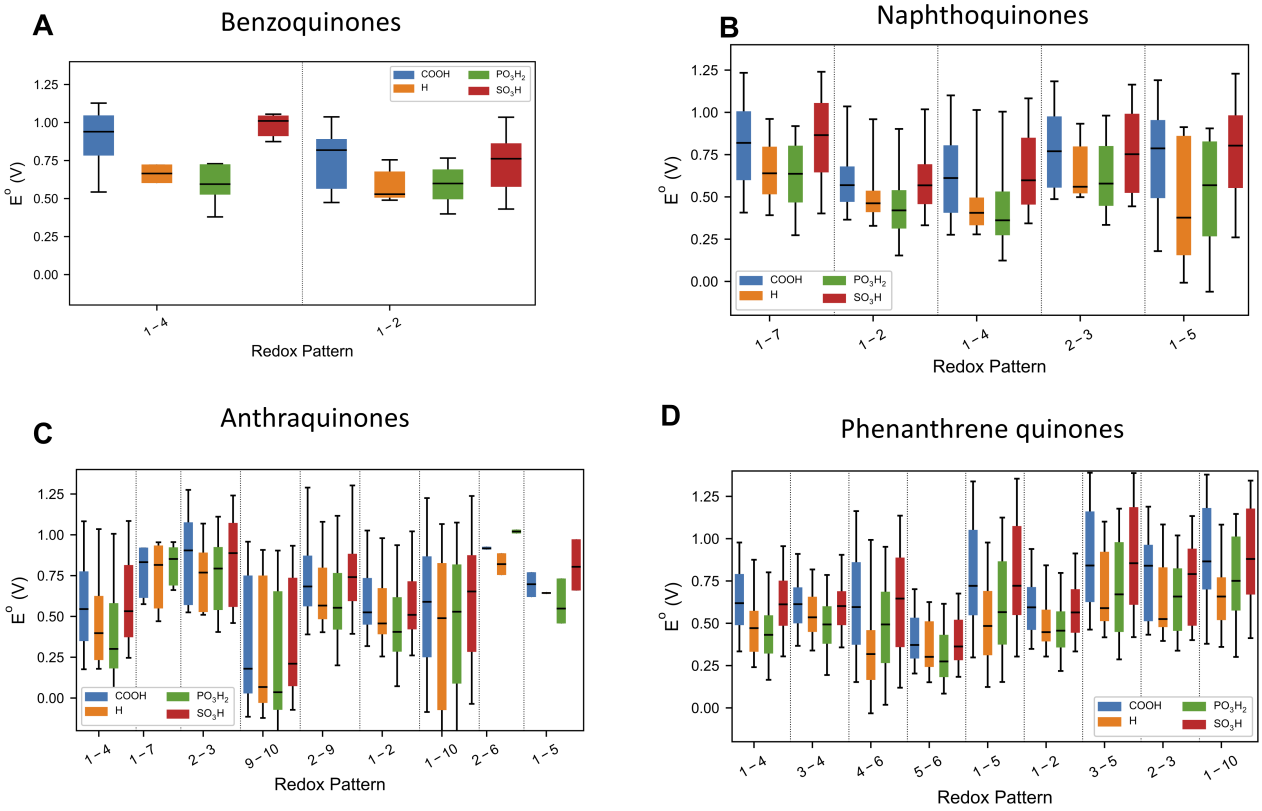

Figure 1: Reduction potential dependence on both relative ketone positions and functional groups. The numbers refer to the topology of the redox-active ketones and correspond to the labels in Scheme 1. The median of each set of data is indicated with a black line. The regions bounded by the colors indicate the range of the 5th and 95th percentile of reduction potentials. The lines extend out to the maximum and minimum reduction potential for each substitution and ketone topology.

are for the anthraquinones (Figure 1C) and phenanthrene-functionalized quinones (Figure 1D). In the former two cases, because the functional groups are much more likely to be close to the redox-active sites of the molecules and thus appear to have a more pronounced effect on the reduction potential. For the two three-ring families of molecules, we see that certain reduction patterns consistently produce higher distributions with 1-7 and 2-3 for anthraquinones and 3-5, 2-3, and 1-10 for the phenanthrene-functionalized quinones.

Relationship between reduction potential and water stability: Computational results

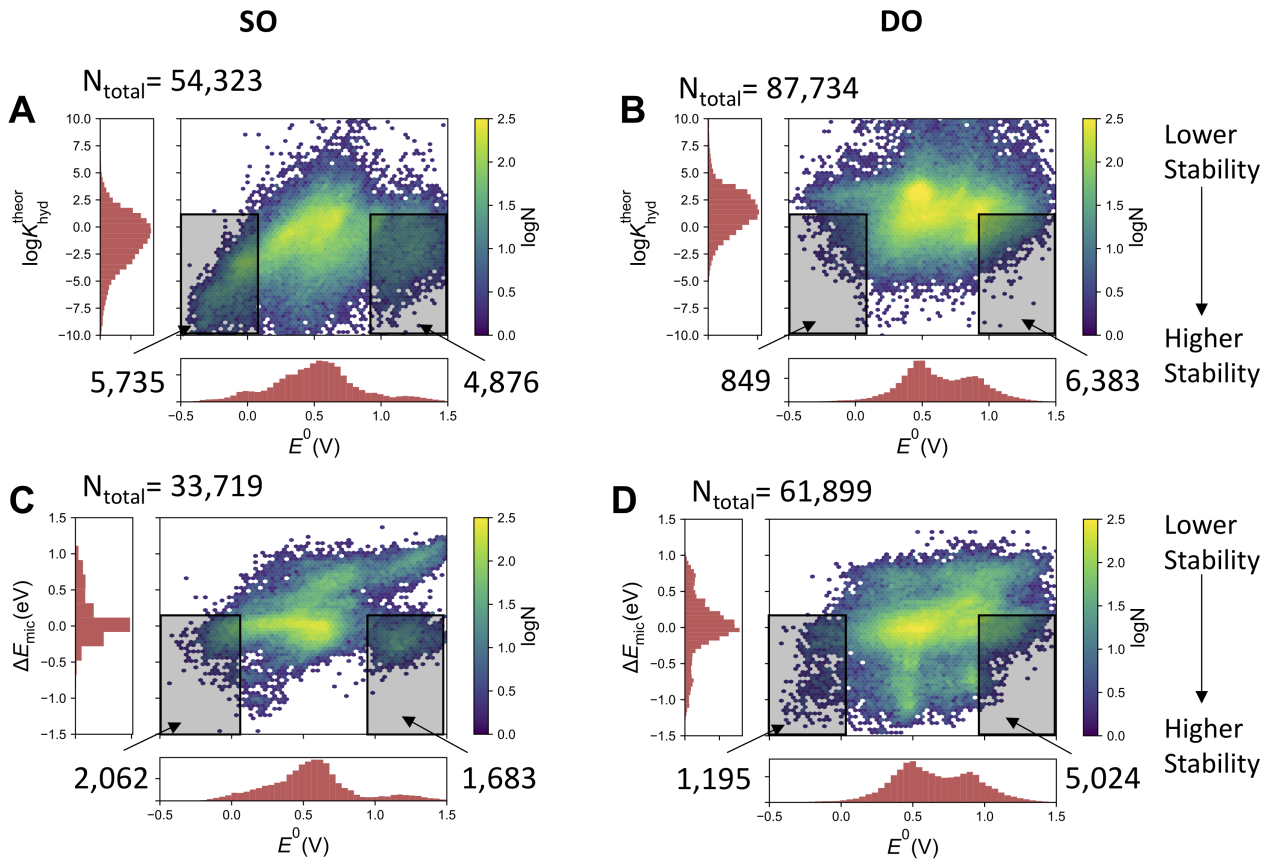

Figure 2: Correlations between calculated nucleophilic attack susceptibility and half-cell reduction potential for quinone-hydroquinone pairs. The quinone pairs are divided into two groups. The SO group contains pairs of molecules where a fully reduced hydroquinone is oxidized through a single two-proton two-electron oxidization to a quinone.The DO group contains pairs of singly two-proton two-electron oxidized quinones that may undergo a second two-proton two-electron oxidation process. N_{total} indicates the number of molecules in each plot. Shaded regions indicate molecules that have both satisfactory reduction potentials to be viable negolytes or posolytes and have relatively high thermodynamic stability with respect to the specified reaction with water.

Having established the structure-property relationships between the quinone functionalization and reduction potential, the relationship between the reduction potential and thermodynamic stability criteria was explored. Two metrics of susceptibility related to the addition of water were considered: $\log K_{\mathrm{hyd}}$ (the calculated base-10 logarithm) and ΔE_{mic} for

a reversible gem-diol formation (Scheme 1C) and irreversible Michael addition/substitution (Scheme 1D), respectively. The calibration results for the calculation of $\log K_{\text{hyd}}$ are in Figure S2. Chemical principles suggest that as molecules become more electron-deficient, both the reduction potential would increase and so would the electrophilicity, thus increasing the susceptibility to nucleophilic attack from a species like water.

The quinone molecules were divided into two groups, motivated by the possibility of discovering a fused-quinone with three separated redox states. Note that in all cases, the fully reduced hydroquinone, which has no ketone groups, is subject to neither gem-diol formation nor the Michael addition. The first group includes quinones that have only a single two-proton two-electron oxidation (referred to in shorthand as **SO** - single oxidation) from its fully reduced form. The second group involves quinones that are the products of a subsequent second oxidation (referred to as **DO** - double oxidation), which means that the oxidized products have four ketone groups. Figures 2A and 2B show the calculated $\log K_{\text{hyd}}$ of the **SO** and **DO** oxidized forms of the pairs, respectively, and Figures 2C and 2D show the same for the Michael addition/substitution energy. We define Michael addition/substitution energy as

$$\Delta E_{mic} = (E(\text{oxidized}) + E(\text{H}_2\text{O}) - E(\text{Michael product})). \quad (1)$$

For the first oxidation (**SO** group), the thermodynamic favorability of nucleophilic attack by water increases with the reduction potential of the molecule (Figure 2A and 2C). This is consistent with the chemical principles argument outlined above that the more electron deficient core will have both a higher reduction potential and be more susceptible to Michael addition. However, for the second two-proton two-electron oxidations, the correlation between both $\log K_{\text{hyd}}$ and ΔE_{mic} and the reduction potential is substantially less pronounced. This seems to indicate that all fused quinones in their fully oxidized state are relatively electron deficient, or at least have an electron deficient spatial region, in terms of having a vulnerable site for water attack. This implies that the development of a fused quinone that is stable is more challenging than a high reduction potential molecule with the same reduction

potential.

Experimental investigation of fused quinone stability

A family of fused quinones was investigated experimentally to both test the validity of the computational studies and also provide guidance for what cutoff criteria should be used for various properties in a virtual screening. The full list of molecules investigated is provided in Table S3 of the Supplementary Material. The molecules in this family in general have a stable, reversible cyclic voltammetry (CV) signal at low potential ($\sim 0.1-0.2$ V), but do not have a reversible peak at high potential (~ 1.0 V). The CVs are provided in Figure S3-S5 in the supplementary material. We focus on alizarin red S (molecule indicated in Figure S7A), which was studied in a full cell. At 50% state of charge, an aliquot was taken and separated with high-performance liquid chromatography. The separated components were detected with mass spectrometry (MS), which allowed for assignment of the molecules present at 50% state of charge.

Molecules were detected in two mass channels. The first detected molecule is the starting material (Figure S6A) with evidence of a small amount of impurity that corresponds a sulfonate functionalization at a different position. The second detected mass (Figure S6B) has a mass consistent with two products: 1) Michael addition to the fully oxidized form of alizarin red S at the 4 position and subsequent tautomerization or 2) Gem-diol formation on the fully oxidized form of alizarin red S, which theoretical calculations predict to be most thermodynamically favored at the 1 position (a smaller third peak is also detected, which is most likely the product of one of these processes on the impurity). When the mode of nucleophilic attack is Michael addition, it is effectively a reduction of the system (Scheme 1D) after tautomerization.

The LC-MS results raise the question on the extent of the vulnerability of the fully-oxidized molecule to Michael attack in the presence of water. It is possible to chemically synthesize the oxidized form of quinizarin (Figure S7 of the Supplementary Material) and

leave it solution overnight. In the presence of H_2SO_4, the molecule decomposes to some extent, but not completely, which implies that the oxidized form is at least stable on a measurable timescale.

For reference, the PM7 COSMO-calculated Michael addition energy to alizarin red S is 0.03 eV, which we use as an upper cutoff for further screening criteria below.

Effects of Michael addition on reduction potential

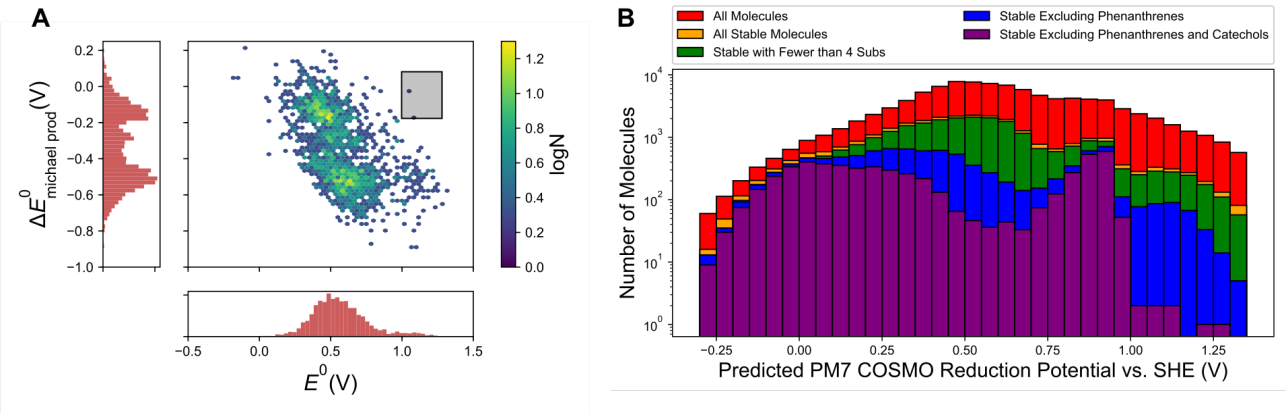

Figure 3: A) Change in the reduction potential of a molecule upon Michael addition, 1763 molecules pictured. The desired region, high potential molecules that show almost no change in reduction potential upon Michael addition, is shaded in the black box and contains only two molecules (sulfonated 1-4 benzoquinones), which are shown in Figure S8. B) Plot of the redox potential distributions of various sets of molecules, as indicated in the legend. Molecules are defined as "stable" if they have the following criteria 1) PM7 COSMO Michael addition energy < 0.03 eV and 2) $\log K_{\text{hyd}} < 1.0$.

Given the theoretical and experimental evidence for the susceptibility of high reduction potential quinones to Michael addition/substitution, the next important question to address is the ultimate effects of Michael addition on battery performance. To investigate this, we found ∼1700 molecules in our database that had been generated through combinatorics that were also Michael addition/substitution products of other molecules in our database and evaluated the reduction potential of these Michael products. The effects of Michael addition/substitution on the reduction potential show a bimodal distribution (3A). The first of these modes clustered around a -0.15 to -0.2 V shift in reduction potential upon Michael

addition. This cluster consists of molecules that maintain the same redox-active topology as before Michael addition and the decrease in the reduction potential simply comes from the increased electron density on the quinone core, due to the electron-donating tendencies of hydroxyl groups. The second cluster of molecules is centered around a -0.5 V shift in reduction potential. These correspond to molecules where the redox pattern is changed, for instance a 1-2 quinone becomes a 1-4 quinone. In both cases, Michael addition will substantially decrease the OCV of any battery that uses the Michael-susceptible molecule as a posolyte, as has been seen in tiron.[6] In addition, the first Michael addition product may also be susceptible to further reactions with water; this would further decrease performance. Thus, it is most reasonable to search for molecules lacking thermodynamic susceptibility to Michael addition to begin with.

Number of promising candidates as a function of reduction potential

Figure 3B shows the number of molecules of particular categories with a Michael addition site that satisfy stability criteria, on a logarithmic scale. The stability criteria that were employed are:

1. Calculated $\log K_{\text{hyd}} < 1.0$, this corresponds the gem-diol form of a molecule being less than 10 times more abundant, in equilibrium, than the oxidized form of the molecule. Although gem-diol formation is still more favored when K_{hyd} is between 1 and 10, the redox-active ketone form may be present in sufficient quantity to give satisfactory battery performance.

2. $\Delta E_{mic} < 0.03$ eV, this cutoff means that the molecule is less susceptible to Michael addition than alizarin red S, which we showed via LC-MS undergoes Michael addition.

At the low reduction potentials (< 0.2 V), hundreds of molecules are calculated to be thermodynamically stable. However, at high reduction potentials (> 0.95 V vs. SHE), the

percentage of stable molecules drops off precipitously, especially if exotic phenanthrene-functionalized molecules or oxidized catechols are excluded. The surviving molecules are enormously rare, numbering in the tens (and are shown in Figures S9 and S10 in the Supplementary Material). Given that there is a mean absolute error associated with the PM7 COSMO calculations of about 0.07 V for reduction potentials and 1.3 log units for $\log K_{\text{hyd}}$ from our calibrated results, it is possible that the molecules that are passing the stability screening are the molecules with larger calculations errors and thus are false positives. Making the criteria more stringent ($\log K_{\text{hyd}} < 0.0$ and $\Delta E_{mic} < 0.00$ eV) dramatically reduces the number of viable molecules (Figure S11). It should be noted that there is a population of about 40,000 pairs, containing mostly exotic phenanthrene-functionalized quinones, with oxidized forms lacking a valid Michael addition site according to the substitution rules we formulated. These are potentially viable, resulting in about 1500 pairs whose oxidized form has a predicted reduction potential > 0.95 V vs. SHE. A sampling of these is enumerated in Figure S12 in the Supplementary Material. These molecules are expected to be challenging to synthesize and it is possible that they are subject to other decomposition mechanisms not considered in this work, but they constitute a substantial fraction of the most promising molecules at this point.

Conclusion

Taking the computational screening and the experimental together, it is not surprising that the highest reduction potential quinone that has been demonstrated with any full cell cycling in acid reported to date has a reduction potential at 0.85 V vs. SHE (DHDMBS).[8] This lies very close to the stability cliff that we observed in our library, which is between 0.90 and 0.95 V. These results have several implications for the future development of an all-organic redox flow battery. We found almost no quinones that are based on currently used backbones with currently employed functional groups that are both high in reduction

potential (leading to > 1.0 V OCV when paired against another quinone) and thermodynamically protected from Michael addition and/or gem-diol formation. Going forward, two pathways for exploration that do not involve fused quinones are apparent: 1) Attempt to synthesize the exotic phenathrene-based quinones (which may be susceptible to other not-yet-observed decomposition mechanisms, see Scheme S1 in the Supplementary Material for another potential mechanism), or 2) employ strategies to mitigate the Michael addition from a kinetics perspective. Our calculations indicate that the thermodynamic susceptibility to Michael substitution is about 0.13 eV less than the thermodynamic susceptibility to Michael addition between potentials of 1.00 and 1.05 V after averaging over all of the R-groups considered in this study. This can be taken a step further, by developing molecules which, while thermodynamically susceptible to Michael addition, may not be kinetically susceptible, through protection with bulky groups. This strategy has the drawback of adding molecular weight and potentially increasing synthetic cost of the molecules. It would also be desirable to screen for this computationally, though transition state searches are expensive. While introducing a bulky functional group to block the Michael addition/substitution site makes sense from a kinetics perspective, it is not clear what strategy might be employed to mitigate the effects of gem-diol formation. The groups could also lead to the stabilization of tertiary carbocations if the molecule is protonated in acidic solution. The formation of these carbocations was recently reported as a key step in the capacity fade mechanism for DHDMBS.[25] Another potential strategy could be to modulate the pKas of the redox-active sites of the reduced form of these couples. This would lead to a "flattening out" of the potential on the Pourbaix diagram at lower pH and could lead to otherwise unpromising molecules at pH = 0 becoming viable at higher values of pH. Finally, it may be necessary to investigate other organic molecule motifs to find molecules that are less susceptible to water attack, while still providing the high reduction potential and energy density.

Experimental Methods

High-resolution LC-MS analysis of alizarin red S decomposition products was performed in the Small Molecule Mass Spectrometry Facility at Harvard on a Bruker Impact II q-TOF with internal calibration by sodium formate clusters. Liquid chromatography was performed on an Agilent 1290 Infinity HPLC using a Allure PFPP column (5 um particle size, 150 x 2.1 mm) at a flow rate of 0.4 mL/min and the following elution conditions were applied (solvent A = 0.1% v/v formic acid in water; solvent B = 0.1% v/v formic acid in acetonitrile): 100% solvent A for 2 min, a gradient increasing from 0% to 15% solvent B in solvent A over 13 min, a gradient increasing to 100% solvent B over 5 min, a gradient decreasing to 0% solvent B in solvent A over 0.1 min, and 100% solvent A for 4.9 min. The ESI mass spectra were recorded in negative ionization mode.

Computational Methods

Library generation

Molecular libraries were generated programmatically, using several aromatic backbones (benzene, naphthalene, and anthracene from a previous study[21] and phenanthrene and tetracene, which are new for this work; see Scheme 1) using the open-source cheminformatics suite RDKit.[26] The previous study[21] showed that the two-proton, two-electron redox processes in benzo-, naphtho-, and anthraquinones can be modulated by changing the number and position of various substituents along with the positions of the redox-active ketones. The results from that work, using single and full substitution patterns, match organic chemistry principles. This suggests that electron-donating groups (EDG) such as -OH and electron-withdrawing groups (EWG) such as -COOH, -SO_3H, -PO_3H_2 can tune E_0 while maintaining high aqueous solubility and synthetic accessibility.

For this work, molecules were generated using all possible substitution patterns for each

of the three electron withdrawing groups alone and in combination with hydroxyls. In addition, the quinone dataset was expanded via intuition-driven suggestions from experimental collaborators. The molecules generated were used as the reduced parts of redox pairs and subject to two-proton, two-electron oxidation reactions. The R-groups that were included for all backbones were carboxylic, hydroxyl, phosphonic, and sulfonic. In addition, for benzoquinones methylimidazolium, methylpyridonium, and tetramethylimidazolium groups were included on benzoquinones based on feedback from experimentalists.

The presence of multiple hydroxyl R-groups implies multiple oxidation patterns for a given molecule, but only one isomer will be thermodynamically predominant at virtually any given redox potential. Redox pairs were stored in a database as objects with pointers to reduced and oxidized molecules, allowing us to build reactivity graphs. The ability to create and track molecular linkages allowed us to book-keep the relationships between the species and to calculate pairwise properties, such as reaction free energies.

The presence of multiple substitutions also expands the idea of blocking of Michael addition. This blockage was less likely to happen in the previous one-substitution studies. However, these substituents are also good leaving groups, so the important quantity to examine is the relative energy of the tetrahedral intermediate of the Michael substitution. If this step in the proposed mechanism is thermodynamically favored, then we assume that substitution is favored overall.

Whereas some of the patterns may appear rare and are thermodynamically unfavorable if alternative oxidations exist, it is important to include them. Otherwise a fraction of the molecules in a reaction graph could be outside the library, and thus completely ignored. In total, 146,857 quinone/hydroquinone pairs were generated. Corresponding gem-diols for each oxidized molecule were also included in the database. We also included decomposition products associated with irreversible Michael addition of water onto α-β unsaturated carbonyls (or γ-δ, *etc.* when available). Depending on the substitution of the β site, two potential pathways are possible:

1. For hydrogen-substituted sites, this reaction results in an intermediate enol, which isomerizes to a reduced, hydroxylated hydroquinone (Figure 1C). Thus, the final product of this reaction is an electrochemically active quinone, although it is in the reduced state, so it needs to be oxidized again to recover the stored charge. However, this molecule can have significantly different electrochemical behavior than the original electrolyte with a much lower potential.

2. For functionalized β sites and depending on the nature of the substituent, the addition can be followed by loss of the R-group and isomerization to hydroquinone. Bulky substituents will have a significant steric effect, increasing the barrier for water addition.

98,043 Michael addition products were generated from these pairs, based on the allowed patterns considered above. Both Michael substitution and Michael addition were allowed.

Electronic structure methods

Quantum chemistry is the bottleneck of this virtual screening study. In the previous study on a select group of singly and fully-substituted quinones (totaling 1710 quinone molecules), plane wave DFT calculations were employed.[21] Here, on a molecular screening study with ∼1,000,000 molecules (considering all of the potential decomposition products that are also considered), lower cost electronic structure methods are needed that also maintain accuracy similar to the previous study. Other recent studies have also demonstrated capability of different levels of DFT (with and without calibration and/or explicit solvation) to estimate the reduction potentials of organic molecules, including quinones.[4,22,27,28]

The calculated reaction energies for both reduction and gem-diol reactions were benchmarked against experimental reduction potentials and gem-diol hydration equilibrium constants (Tables S1 and S2 of the Supplementary Material) at several different levels of electronic structure theory. Benchmarking studies have been performed at the following levels of theory: PBE/6-31G(d) optimization and B3LYP/6-31G(d) optimization, B3LYP/6-

311+G(d,p) gas-phase single point (at PBE/6-31G(d) gas-phase geometries), and B3LYP/6-311+G(d,p) PCM single point energies using the CPCM as implemented in QChem 4.0 with water as the solvent.[29] The PBE/6-31G(d) optimizations were implemented using TeraChem.[30,31] Semi-empirical methods were also benchmarked; the energies were computed at both the PM7 and PM7 with the COSMO solvation model with water as a solvent (referred to as PM7 and PM7 COSMO, respectively).

We have performed a benchmark study of these cheaper methods and compared their ability to predict the reduction potential and hydration equilibrium constant.

Using a well-characterized experimental set of reduction potential measurements, we tested the calibration scheme by comparing the zero-temperature reaction electronic energy for the reduction (E_{red}) with experimentally-determined quinone reduction potentials (E^0) in aqueous solution (pH = 0) at 298 K. Notwithstanding computational affordability, all the methods are close in the accuracy of their predictions (see Supplementary Figure S1).

Similarly, we carried out carried out a calibration of the hydration equilibrium constant by mapping zero-temperature energy differences for the carbonyl hydration reaction (E_{hyd}) with experimentally determined equilibrium constants (K_{hyd}) in water at 298 K.

When considering both the accuracy and computational cost of the various methods, the PM7 COSMO optimization has the best balance. B3LYP/6-311+G(d,p) (PCM) gives a marginally lower deviation on the calibration set, but does not justify the extra cost here.

For computing the vulnerability to Michael addition/substitution, we did not have a body of data against which to calibrate. However, we can use the results of tiron and alizarin red S to gain a sense of scale. At the PM7 COSMO level of theory, the Michael addition free energy for water addition to tiron is 0.25 eV and that of alizarin red S is 0.03 eV.

Supplementary Material

The supplementary material contains plots showing the calibration of the reduction potential and $\log K_{\mathrm{hyd}}$ at different levels of electronic structure theory, the raw data that are used to calibrate the reduction potential and $\log K_{\mathrm{hyd}}$, CVs and the calculated thermodynamic stability of the alizarin family, the synthesis and NMR stability study of quinizarin, lists of high-potential molecules that pass various stability criteria, results of screening from stricter stability criteria, and a scheme for a potential ring-opening mechanism not fully explored in this paper.

Acknowledgments

Research at Harvard was supported by the Innovation Fund Denmark via the Grand Solutions project "ORBATS" file nr. 7046-00018B, U.S. DOE ARPA-E award DE-AR0000767, and the Massachusetts Clean Energy Technology Center. This work was also supported by the National Science Foundation through grant No. CBET-1509041. A.A.-G. is very thankful to the Canadian Institute for Advanced Research (CIFAR) for their generous support and collaborations. A. A.-G. Thanks Anders G. Frøseth for the generous support of his work. A. A.-G. acknowledges support from the Canada 150 Research Chairs Program.

References

(1) Brushett, F. R.; Vaughey, J. T.; Jansen, A. N. An All-Organic Non-aqueous Lithium-Ion Redox Flow Battery. *Adv. Energy Mater.* **2012**, *2*, 1390–1396.

(2) Huskinson, B.; Marshak, M. P.; Suh, C.; Er, S.; Gerhardt, M. R.; Galvin, C. J.; Chen, X.; Aspuru-Guzik, A.; Gordon, R. G.; Aziz, M. J. A Metal-Free Organic-Inorganic Aqueous Flow Battery. *Nature* **2014**, *505*, 195–198.

(3) Lin, K.; Chen, Q.; Gerhardt, M. R.; Tong, L.; Kim, S. B.; Eisenach, L.; Valle, A. W.; Hardee, D.; Gordon, R. G.; Aziz, M. J.; Marshak, M. P. Alkaline quinone flow battery. *Science* **2015**, *349*, 1529–1532.

(4) Lin, K.; Gómez-Bombarelli, R.; Beh, E. S.; Tong, L.; Chen, Q.; Valle, A.; Aspuru-Guzik, A.; Aziz, M. J.; Gordon, R. G. A redox-flow battery with an alloxazine-based organic electrolyte. *Nat. Energy* **2016**, *1*, 16102.

(5) Liu, T.; Wei, X.; Nie, Z.; Sprenkle, V.; Wang, W. A Total Organic Aqueous Redox Flow Battery Employing a Low Cost and Sustainable Methyl Viologen Anolyte and 4-HO-TEMPO Catholyte. *Adv. Energy Mater.* **2016**, *6*, 1501449–n/a, 1501449.

(6) Yang, B.; Hoober-Burkhardt, L.; Wang, F.; Surya Prakash, G. K.; Narayanan, S. R. An Inexpensive Aqueous Flow Battery for Large-Scale Electrical Energy Storage Based on Water-Soluble Organic Redox Couples. *J. Electrochem. Soc.* **2014**, *161*, A1371–A1380.

(7) Janoschka, T.; Martin, N.; Hager, M. D.; Schubert, U. S. An Aqueous Redox-Flow Battery with High Capacity and Power: The TEMPTMA/MV System. *Angew. Chem. Int. Ed. 55*, 14427–14430.

(8) Hoober-Burkhardt, L.; Krishnamoorthy, S.; Yang, B.; Murali, A.; Nirmalchandar, A.; Prakash, G. K. S.; Narayanan, S. R. A New Michael-Reaction-Resistant Benzoquinone for Aqueous Organic Redox Flow Batteries. *J. Electrochem. Soc.* **2017**, *164*, A600–A607.

(9) Hu, B.; DeBruler, C.; Rhodes, Z.; Liu, T. L. Long-Cycling Aqueous Organic Redox Flow Battery (AORFB) toward Sustainable and Safe Energy Storage. *J. Am. Chem. Soc.* **2017**, *139*, 1207–1214.

(10) Beh, E. S.; De Porcellinis, D.; Gracia, R. L.; Xia, K. T.; Gordon, R. G.; Aziz, M. J. A Neutral pH Aqueous Organic-Organometallic Redox Flow Battery with Extremely High Capacity Retention. *ACS Energy Lett.* **2017**, *2*, 639–644.

(11) Kowalski, J. A.; Casselman, M. D.; Kaur, A. P.; Milshtein, J. D.; Elliott, C. F.; Modekrutti, S.; Attanayake, N. H.; Zhang, N.; Parkin, S. R.; Risko, C.; Brushett, F. R.; Odom, S. A. A Stable Two-electron-donating Phenothiazine for Application in Non-aqueous Redox Flow Batteries. *J. Mater. Chem. A* **2017**, *5*, 24371–24379.

(12) Duan, W. et al. "Wine-Dark Sea" in an Organic Flow Battery: Storing Negative Charge in 2,1,3-Benzothiadiazole Radicals Leads to Improved Cyclability. *ACS Energy Lett.* **2017**, *2*, 1156–1161.

(13) Yang, Z.; Tong, L.; Tabor, D. P.; Beh, E. S.; Goulet, M.-A.; De Porcellinis, D.; Aspuru-Guzik, A.; Gordon, R. G.; Aziz, M. J. Alkaline Benzoquinone Aqueous Flow Battery for Large-Scale Storage of Electrical Energy. *Adv. Energy Mater. 8*, 1702056.

(14) Kwon, G.; Lee, S.; Hwang, J.; Shim, H.-S.; Lee, B.; Lee, M. H.; Ko, Y.; Jung, S.-K.; Ku, K.; Hong, J.; Kang, K. Multi-redox Molecule for High-energy Redox Flow Batteries. *Joule* **2018**,

(15) Hollas, A.; Wei, X.; Murugesan, V.; Nie, Z.; Li, B.; Reed, D.; Liu, J.; Sprenkle, V.; Wang, W. A Biomimetic High-capacity Phenazine-based Anolyte for Aqueous Organic Redox Flow Batteries. *Nat. Energy* **2018**, *3*, 508–514.

(16) Kwabi, D. G.; Lin, K.; Ji, Y.; Kerr, E. F.; Goulet, M.-A.; De Porcellinis, D.; Tabor, D. P.; Pollack, D. A.; Aspuru-Guzik, A.; Gordon, R. G.; Aziz, M. J. Alkaline Quinone Flow Battery with Long Lifetime at pH 12. *Joule* **2018**, in press, DOI: 10.1016/j.joule.2018.07.005.

(17) Wedege, K.; Dražević, E.; Konya, D.; Bentien, A. Organic Redox Species in Aqueous Flow Batteries: Redox Potentials, Chemical Stability and Solubility. *Sci Rep.* **2016**, *6*, 39101.

(18) Carretero-Gonzalez, J.; Castillo-Martinez, E.; Armand, M. Highly water-soluble three-

redox state organic dyes as bifunctional analytes. *Energy Environ. Sci.* **2016**, *9*, 3521–3530.

(19) Huskinson, B.; Marshak, M.; Aziz, M. J.; Gordon, R. G.; Aspuru-Guzik, A.; Er, S.; Suh, C.; Tong, L.; Lin, K. Quinone and Hydroquinone Based Flow Battery. Patent Application US20160248114A1, 2016.

(20) Gerhardt, M. R.; Tong, L.; Gómez-Bombarelli, R.; Chen, Q.; Marshak, M. P.; Galvin, C. J.; Aspuru-Guzik, A.; Gordon, R. G.; Aziz, M. J. Anthraquinone Derivatives in Aqueous Flow Batteries. *Advanced Energy Materials* **2017**, *7*, 1601488–n/a, 1601488.

(21) Er, S.; Suh, C.; Marshak, M. P.; Aspuru-Guzik, A. Computational Design of Molecules for an All-quinone Redox Flow Battery. *Chem. Sci.* **2015**, *6*, 885–893.

(22) Pineda Flores, S. D.; Martin-Noble, G. C.; Phillips, R. L.; Schrier, J. Bio-Inspired Electroactive Organic Molecules for Aqueous Redox Flow Batteries. 1. Thiophenoquinones. *J. Phys. Chem. C* **2015**, *119*, 21800–21809.

(23) MOPAC2016, James J. P. Stewart, Stewart Computational Chemistry, Colorado Springs, CO, USA, HTTP://OpenMOPAC.net (2016).

(24) Klamt, A. and Schuurmann, G., COSMO: A New Approach to Dielectric Screening in Solvents with Explicit Expressions for the Screening Energy and its Gradient. *J. Chem. Soc., Perkin Trans. 2* **1993**, 799–805.

(25) Murali, A.; Nirmalchandar, A.; Krishnamoorthy, S.; Hoober-Burkhardt, L.; Yang, B.; Soloveichik, G.; Prakash, G. K. S.; Narayanan, S. R. Understanding and Mitigating Capacity Fade in Aqueous Organic Redox Flow Batteries. *J. Electrochem. Soc.* **2018**, *165*, A1193–A1203.

(26) Landrum, G. RDKit: Open-source cheminformatics. `http://www.rdkit.org`.

(27) Huynh, M. T.; Anson, C. W.; Cavell, A. C.; Stahl, S. S.; Hammes-Schiffer, S. Quinone 1 e- and 2 e-/2 H+ Reduction Potentials: Identification and Analysis of Deviations from Systematic Scaling Relationships. *J. Am. Chem. Soc.* **2016**, *138*, 15903–15910.

(28) Kim, H.; Goodson, T.; Zimmerman, P. M. Achieving Accurate Reduction Potential Predictions for Anthraquinones in Water and Aprotic Solvents: Effects of Inter- and Intramolecular H-Bonding and Ion Pairing. *J. Phys. Chem. C.* **2016**, *120*, 22235–22247.

(29) Shao, Y. et al. Advances in molecular quantum chemistry contained in the Q-Chem 4 program package. *Mol. Phys.* **2015**, *113*, 184–215.

(30) TeraChem v 1.9, PetaChem, LLC (2009,2015). See http://www.petachem.com.

(31) Ufimtsev, I. S.; Martinez, T. J. Quantum Chemistry on Graphical Processing Units. 3. Analytical Energy Gradients, Geometry Optimization, and First Principles Molecular Dynamics. *J. Chem. Theory Comput.* **2009**, *5*, 2619–2628.